

# DNN Task Assignment in UAV Networks: A Generative AI Enhanced Multi-Agent Reinforcement Learning Approach

Xin Tang, Qian Chen, Wenjie Weng, Binhan Liao, Jiacheng Wang, Xianbin Cao, Xiaohuan Li

**Abstract**—Unmanned Aerial Vehicles (UAVs) possess high mobility and flexible deployment capabilities, prompting the development of UAVs for various application scenarios within the Internet of Things (IoT). The unique capabilities of UAVs give rise to increasingly critical and complex tasks in uncertain and potentially harsh environments. The substantial amount of data generated from these applications necessitates processing and analysis through deep neural networks (DNNs). However, UAVs encounter challenges due to their limited computing resources when managing DNN models. This paper presents a joint approach that combines multiple-agent reinforcement learning (MARL) and generative diffusion models (GDM) for assigning DNN tasks to a UAV swarm, aimed at reducing latency from task capture to result output. To address these challenges, we first consider the task size of the target area to be inspected and the shortest flying path as optimization constraints, employing a greedy algorithm to resolve the subproblem with a focus on minimizing the UAV's flying path and the overall system cost. In the second stage, we introduce a novel DNN task assignment algorithm, termed GDM-MADDPG, which utilizes the reverse denoising process of GDM to replace the actor network in multi-agent deep deterministic policy gradient (MADDPG). This approach generates specific DNN task assignment actions based on agents' observations in a dynamic environment. Simulation results indicate that our algorithm performs favorably compared to benchmarks in terms of path planning, Age of Information (AoI), energy consumption, and task load balancing.

**Index Terms**—task assignment, path planing, UAV networks, generative diffusion model (GDM), multi-agent deep determinis-

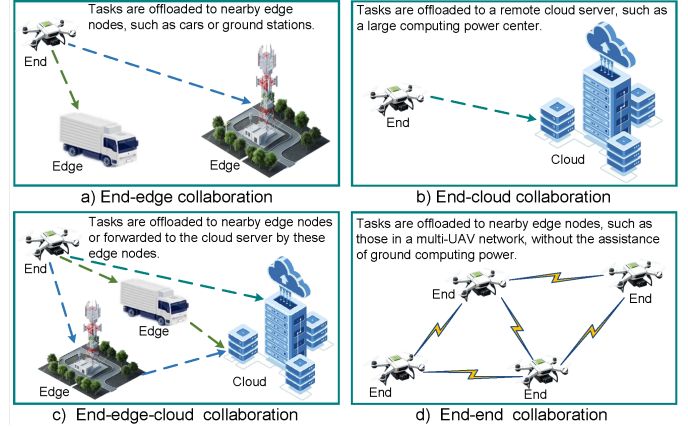


Fig. 1. Four task assignment models.

tic policy gradient (MADDPG), MEC (MEC).

## I. Introduction

### A. Background research

Advancements in Unmanned Aerial Vehicles (UAVs) technology have led to their increasing use across various civil and military domains, including aerial object detection, swift rescue operations in disaster-stricken areas [1], [2], emergency scenarios [3], and extensive agriculture [4]. Unlike traditional Internet of Things (IoT) devices [5], UAVs offer not only lower costs but also superior mobility and enhanced data collection capabilities [6]. While UAVs are well-suited for the critical and complex tasks mentioned, managing the substantial data they generate remains a challenge [7]. With the rise of artificial intelligence (AI), deep neural networks (DNNs) have been proposed to handle the extensive data produced [8]. Despite their efficiency in processing data, DNNs require significant resources due to their intricate structure and high performance demands. General methodologies segmented DNN models by layers, treating each layer as the primary computational unit, which often led to inefficiencies in collaborative inference due to the substantial computational demands of certain layers. Given the size and cost constraints of UAVs, their power supply is often limited, and their computing capacity is relatively low. Generally, there are two primary approaches to tackle this issue. One approach involves deploying lightweight models on UAVs, which reduces computational demands and

This work was supported in part by the National Natural Science Foundation of China under Grant U22A2054, in part by the Guangxi Natural Science Foundation of China under Grant 2024JJA170165, and in part by the Graduate Study Abroad Program of Guilin University of Electronic Technology under Grant GDYX2024001. (Corresponding author: Xiaohuan Li).

Xin Tang is with the Guangxi University Key Laboratory of Intelligent Networking and Scenario System (School of Information and Communication, Guilin University of Electronic Technology), Guilin 541004, China, and also with the College of Computing and Data Science, Nanyang Technological University, 639798, Singapore (e-mails: tangx@mails.guet.edu.cn).

Qian Chen is with the School of Architecture and Transportation Engineering, Guilin University of Electronic Technology, Guilin 541004, China (e-mails: chenqian@mails.guet.edu.cn).

Wenjie Weng, Binhan Liao and Xiaohuan Li are with the Guangxi University Key Laboratory of Intelligent Networking and Scenario System (School of Information and Communication, Guilin University of Electronic Technology), Guilin 541004, China, and also with National Engineering Laboratory for Comprehensive Transportation Big Data Application Technology (Guangxi), Nanning 530001, China (e-mails: wwjdzsyx@163.com; binhanliaoguet@163.com; lxhguet@guet.edu.cn).

Jiacheng Wang is with the College of Computing and Data Science, Nanyang Technological University, 639798, Singapore (e-mail: jiacheng.wang@ntu.edu.sg).

Xianbin Cao is with the School of Electronic and Information Engineering and the Key Laboratory of Advanced Technology of Near Space Information System, Ministry of Industry and Information Technology of China, Beihang University, Beijing 100191, China (e-mail: xbcao@buaa.edu.cn).

TABLE I  
COMPARISON BETWEEN RELATED WORKS AND OUR PROPOSED

Ref.	Architecture	Adaptive partitioning	Trajectory Planning	Latency	Energy consumption	Reliability	Age of information
[10]	End to edge	✓		✓			
[11]	End to end	✓		✓		✓	
[12]	End to end		✓	✓		✓	
[13]	End to end / edge			✓	✓		
[14]	End to end			✓	✓	✓	
[15]	End to end / cloud	✓		✓			
[16]	End to edge		✓				✓
[17]	End to end			✓			
[18]	End to end / edge		✓	✓			
[9]	End to end	✓		✓			
Proposed	End to end	✓	✓	✓	✓	✓	✓

inference latency but sacrifices accuracy [9]. However, executing computation-intensive tasks independently with a single UAV presents significant challenges in achieving low latency and high inference accuracy. Another approach is to consider designing from the perspective of the end-edge-cloud network architecture. This kind of approach is to enable real-time processing with high accuracy on UAVs, leveraging cloud and edge servers to support UAV computations.

Recent studies have shifted focus from relying solely on the cloud or a single edge device, such as a UAV, to harnessing the combined capabilities of both robust external cloud resources and edge servers for the collaborative execution of complex task. This collaborative approach can generally be categorized into four types of collaborative intelligence: End-edge [16], [19], End-cloud [15], [20], End-edge-cloud [21], [22] and End-end [14], [23]. While the first three types effectively mitigate extensive original data transmission to minimize latency and uphold high accuracy, such as DNN inference ability, they may still encounter significant processing latencies and potential failures when implemented in UAV contexts due to the instability of air-to-ground communication links, particularly in real-time dynamic applications. As end resources become increasingly abundant, some researchers have explored the possibility of conducting collaborative DNN inference across multiple end devices—specifically UAVs in the scenario under consideration—without dependence on edge servers or the cloud, termed End-end. This model aligns seamlessly with UAV operations, which typically involve task execution within UAV swarms, thereby reducing execution time and enhancing fault tolerance. Fig. 1 depicts the four conventional paradigms.

### B. Motivation and challenges

Although current research on collaborative DNN inference within multi-UAV offers a promising approach for processing DNN-based tasks, significant issues still need to be resolved [9]–[15], [17], [18].

The primary challenge is that conventional scene data collection and monitoring tasks rely on staged task processing. For example, in [10], [24], the methods involve an initial phase of task planning, followed by data collection, and concluding with online or offline processing of related tasks, such as target detection and positioning. This sequential approach is evidently inadequate for meeting the real-time requirements of

sudden events or emergency scenarios. Moreover, the limited computational power, battery life, and other onboard resources of UAVs further constrain their ability to perform real-time tasks effectively.

Secondly, when DNN tasks need to be offloaded, many studies explore the transfer of intermediate data to ground nodes [13], [15], [18]. However, non-line-of-sight communication and the high relative mobility between UAVs and ground nodes—especially dynamic nodes—introduce significant uncertainty into the offloading process. Additionally, existing methods for offloading computationally intensive tasks, such as heuristic-based, decomposition-based [10], and game-based approaches [20], [25], typically require numerous iterations to converge to a satisfactory and stable assignment decision. This iterative decision-making process is often impractical for latency-sensitive tasks and energy-constrained systems.

Thirdly, non-uniformities in the processing pipeline of DNN-based tasks are apparent. To elucidate this, we conduct a pilot study analyzing layer-wise execution latency, intermediate output data size, and computational demands for Yolov5 [26], AlexNet [27], and VGG16 [28]. The results, shown in Fig. 2, demonstrate most of the computational cost is concentrated in the first half of the DNN, with considerable variability in latency, output data size, and computation across different layers of these DNNs. This underscores the need for uniform task division. Arbitrary division can lead to significant imbalances in task assignment among UAVs, which may adversely affect the operational efficiency and survival time of the multi-UAV, thereby hindering its overall effectiveness in multi-UAV operations [12]. To delineate the differences between the proposed DNN task assignment strategy and existing studies in this field, a comparison of various works is presented in Table I. Performance metrics meeting the specified criteria are indicated with a ✓.

### C. Summary of contributions

In this paper, our approach presents several distinctions from prior research. Specifically, we develop a collaborative inference model system for multi-UAV network. The model processes image classification requests by distributing and assigning the inference computations to the most suitable UAVs to minimize collaborative inference latency. This approach also considers each UAV’s memory footprint, computing resources, energy consumption, and the number of layers

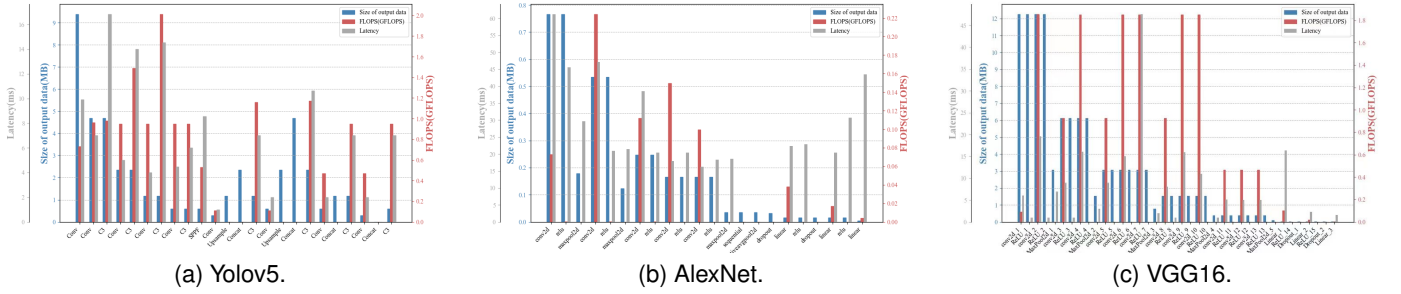


Fig. 2. The computational complexity, processing latency, and output data size of each layer of different types of DNNs.

they can execute. Moreover, our method introduces a finer-grained task division compared to previous research. Our main contributions are outlined as follows

- We propose a mother-and-child UAV system for regional inspection tasks. This system employs a high-altitude platform (HAP), such as an airship, equipped with multiple UAV launchers. From this HAP, several small UAVs are launched and networked to support collaborative multi-UAV tasks. Then we design DNN tasks directly on UAVs, performing inference independently of the ground base station. This approach enhances the scalability of the system. Furthermore, we propose a novel greedy algorithm for UAV path planning that utilizes a fitness function to minimize flying distance, taking into account the varying sizes of tasks.
- We formulate the long-term optimization problem of joint task division, task completion latency, energy consumption, and UAV selection in a multi-UAV network as a Mixed Integer Nonlinear Program. Subsequently, we introduce a multi-agent reinforcement learning (MARL) algorithm based on a generative diffusion model (GDM) to address this optimization problem. Our work tackles constraints related to task completion latency and power while also considering the number of UAVs, AoI of DNN task, cache capacity, and energy consumption limitations. Notably, our research is the first to integrate a GDM into the MARL framework specifically for multi-UAV networks.
- The proposed algorithm leverages an innovative application of a GDM to determine optimal DNN task assignment decisions. We use the reverse denoising process of the GDM instead of the actor network of the multi-agent deep deterministic policy gradient (MADDPG) to generate specific DNN task assignment actions based on the agent's observations in a dynamic environment. The GDM functions by sequentially reducing noise through a series of denoising steps, thereby extracting optimal decisions from an initial state of Gaussian noise. By decomposing complex computations into simpler subtasks, we achieve substantial reductions in latency and enhance the overall efficiency of collaborative DNN task.
- We assess the effectiveness of the proposed DNN task assignment algorithm through numerical experiments, analyzing its performance across various simulation set-

tings. This evaluation includes comparisons with several benchmark algorithms to highlight its strengths and advantages, demonstrating the superior performance of our approach.

The organization of this paper is as follows: Section II reviews the related works. the system model is formulated in Section III. Section IV describes the proposed problem. Section V formulates the UAV's path planning approach. In Section VI describes the GDM-MADDPG approach for DNN task assignment. Section VII presents the simulation results, and the paper concludes in Section VIII.

## II. Related works

Henceforth, we summarize contributions of the related works and discuss the distinctions between prior research and our methodology.

### A. Edge intelligent for DNN task

DNN task partition represents a significant research challenge that entails dividing a DNN into several segments and distributing these segments across designated locations. The existing works provide valuable insights to support efficient DNN inference task. The authors in [29] present a joint design for task partitioning and offloading in DNN-enabled edge computing, involving a server and multiple devices. In [30], the authors propose a multi-task learning-based asynchronous advantage actor-critic approach, and explore distributed DNN inference through fine-grained model partitioning in edge computing. These studies overlook the unique characteristics of multi-UAV networks, such as the mobility of edges and ground nodes. The authors in [31] explore accelerating DNN-based task processing in vehicular edge computing through task partitioning and offloading. In [17], the authors propose an efficient allocation strategy using RL, and investigate fast DNN inference in UAV swarms through multi-UAV collaboration. The studies have not addressed the adaptation challenges associated with the partitioning of DNN tasks. The authors in [32] present a novel technique for partitioning DNNs into multiple segments for processing on both local devices and powerful nodes in fog networks. However, these studies oversight may result in decreased network reliability in certain resource-constrained node networks due to suboptimal task assignment within the DNN.

### B. MARL for task offloading

MARL enables each agent to optimize its policy through observations of both the environment and the policies of other agents [33], [34]. Many existing MARL-based approaches significantly enhance task offloading efficiency within dynamic networks [19], [35]. The authors in [36] propose a dedicated actor neural network for coordination and a scalable training algorithm for UAV-aided MEC task offloading. In [37], the authors present a DRL-based joint secure offloading and resource allocation scheme for vehicular edge computing networks. Task processing latency is a critical metric for evaluating the performance of task offloading strategies. The studies have given limited attention to this aspect. In [38], the authors propose an adversarial MARL scheme for secure computational offloading and resource allocation in a multi-UAV-assisted MEC system. The authors in [39] present a mobility-aware service offloading and migration scheme with Lyapunov optimization and a MADDPG algorithm. In [40], a distributed task offloading strategy based on MARL is introduced to optimize task allocation efficiently. The authors in [41] focus on optimizing task offloading and UAV trajectory under energy and queue latency constraints. However, most of these studies concentrate on optimizing network performance metrics, including task completion latency and energy consumption. Our research emphasizes DNN inference services, where the AoI for DNN tasks as a critical performance metric.

### C. GAI for UAV networks

GAI has the potential to effectively overcome the limitations of conventional AI and can be applied to optimize UAV networks, particularly in improving transmission rates, communication capacities, and energy efficiency [42]–[44]. In [45], the authors present a radio propagation model with a conditional generative adversarial network. The authors in [46] introduce a two-stage generative neural network to predict link states and generate path losses, latencies, and angles of arrival and departure in millimeter wave communication for UAVs. The authors in [47] explore the long-term optimization of joint task offloading and resource allocation in a multi-access edge computing network for UAVs. In [48], the authors present a hierarchical aerial computing system where UAVs collect tasks from ground devices and offload them to HAPs. Different from the above schemes, we contribute to the existing literature by presenting a novel application of GDM in the context of DNN task assignment decision. Our approach incorporates a path planning, GDM-based MARL decision-making framework specifically tailored for multi-UAV networks. This methodology aims to minimize the cost associated with DNN task completion while ensuring the system’s reliability.

## III. System model

In this section, we first present the considered network architecture, then detailly introduce the DNN task model, communication model, mobile model, AoI model, and energy consumption model, respectively.

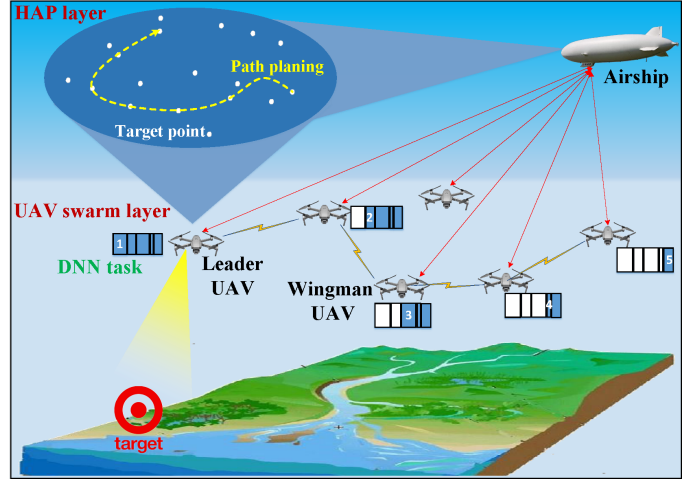


Fig. 3. Network architecture.

### A. Network architecture

The network architecture is primarily composed of an HAP layer and a UAV swarm layer, as illustrated in Fig. 3. The HAP layer consists of a tethered platform with extensive computing and communication capabilities, such as an airship. This platform exchanges information with UAVs via wireless links to facilitate model training [49] and path planning (see Section V). The UAV swarm comprises a leader UAV and multiple wingman UAVs. All UAVs are isomorphic, with the total number of UAVs being  $n = \{1, 2, \dots, N\}$ , and each is equipped with trained DNN models. The leader UAV receives path planning results transmitted by the airship and operates according to the predetermined route. It is also responsible for collecting and processing images and point cloud data of the target area, including tasks such as target detection and mapping. Thus, it functions as both a task producer and executor, as well as a decision-maker for task assignment. The wingman UAVs primarily execute the tasks offloaded by the leader UAV, with the assignment of DNN tasks between wingman UAVs being streamlined. The leader UAV evaluates the task size and the remaining resource status of the wingman UAVs to determine whether to offload tasks. Therefore, to prevent task overload on the UAVs, extend the operational lifespan of the UAV swarm, and enhance the timeliness of task processing and network stability, efficient task assignment decisions for the UAV swarm are particularly crucial.

### B. DNN Task Model

The area where the task is performed in this paper consists of  $q$  target area center coordinate points, denoted as  $q = 1, 2, \dots, \mathbb{W}$ , and the sequence of the UAV inspection target points is represented as  $\mathbf{q}(q) = [q(1), \dots, q(\mathbb{W})]$ . The task data size in the target area is  $\ell_q = \{1, \dots, \mathbb{L}_{\mathbb{W}}\}$ . Assume that the number of DNN tasks in each synchronization cycle is  $i = \{1, 2, \dots, I\}$ , the DNN type is  $\kappa = \{1, \dots, \mathbb{K}\}$  (such as Yolov5 [26], VGG16 [28], etc.). The DNN model typically comprises  $l$  layers, denoted as  $l = \{1, 2, \dots, L\}$ . Each layer has a cache capacity  $m_{i,l}$  and a computing requirement  $c_{i,l}$ ,

represented by a tuple  $(m_{i,l}, c_{i,l})$ .  $l_\kappa = \{1, 2, \dots, L_\kappa\}$  represents a set of layers associated with a specific type of DNN task, including convolutional and pooling layers for feature extraction, as well as fully connected layers for classification [8]. The DNN task is decomposed into multiple subtasks for serial processing, with each wingman UAV serving as an execution stage in this serial processing. This approach allows each subtask to offload and transfer intermediate results among different wingman UAVs without requiring the processing of the entire task, thereby enhancing the computational efficiency and real-time performance of computationally intensive and latency-sensitive tasks [11].

In response to such practical needs, determining the optimal split point of the task is crucial in DNN task assignment. Assume that the split point of the  $i$ -th DNN task model is  $P_{i,n'}$ , and  $n' \in \{1, 2, \dots, N-1\}$  represents the number of subtasks generated after the DNN task model is divided into blocks, with its size depending on the initial task data size. Based on the size of the task data, we can categorize the task assignment modes into swarm assignment, partial assignment, and binary assignment. Swarm assignment indicates that the DNN task is processed serially through pipeline assignment across all wingman UAVs. Partial assignment means that the DNN task is processed serially through pipeline assignment among some wingman UAVs. Binary assignment entails that the DNN task is completely offloaded to a single wingman UAV for processing. The DNN task assignment mode  $M$  is expressed as follows

$$M = f(k, \ell, \tau_i^{max}, O), \quad (1)$$

where  $f(\cdot)$  represents the function that determines the task assignment mode (see Section VI).  $\tau_i^{max}$  denotes the maximum latency allowed for the total completion time of each task, and  $O$  represents the state space of the wingman UAV.

### C. Communication Mode

DNN task assignment is performed within the UAV swarm, and during the task execution, the UAV swarm maintains a fixed formation flying. At time slot  $t$ , the coordinates of each UAV are designated as  $\mathcal{P}^n = [x_t^n, y_t^n, z_t^n]$ , and the distance between the two UAVs is defined as follows

$$d_t^{n,n+1} = \sqrt{\|\mathcal{P}^n - \mathcal{P}^{n+1}\|^2}. \quad (2)$$

The UAV-to-UAV data link utilizes line-of-sight communication, and its channel model is described by the Close-in (CI) free space reference model [35], [43]. The path loss is expressed as follows

$$PL_{CI}(d_t^{n,n+1}, f) = PL_{FS,ref}(f) + 10n_{CI} \log_{10} \left( d_t^{n,n+1} \right) + \xi_{\sigma, CI}, \quad (3)$$

where  $PL_{FS,ref}(f)$  represents the free space path loss per unit length,  $n_{CI}$  is the path loss index, and  $\xi_{\sigma, CI}$  is the shadow fading parameter, which is typically assumed to follow a zero-mean Gaussian distribution.

The signal-to-noise ratio between the two UAVs is formulated as follows

$$SINR_t^{n,n+1} = \frac{P_n - PL_{CI}(d_t^{n,n+1}, f)}{P_I + P_N}, \quad (4)$$

where  $P_n$  is the information transmission power of the UAV,  $P_I$  is the interference power, and  $P_N$  is the noise power, denoted as  $P_N = kBT$ , where  $k$  is the Boltzmann constant,  $B_n$  is the bandwidth of the channel, and  $T$  is the absolute temperature.

Therefore, the data transmission rate between the UAVs can be expressed as follows

$$r_t^{n,n+1} = B_n \log_2 \left( 1 + SINR_t^{n,n+1} \right). \quad (5)$$

### D. Mobile Mode

Let  $\varphi_q$  denote the binary decision variable for the inspection target point  $\mathbf{g}_{q(q)}$ ; specifically, when the target point  $\mathbf{g}_{q(q)}$  is inspected by the UAV,  $\varphi_q$  is equal to 1. Otherwise,  $\varphi_q$  is equal to 0. After the UAV swarm collects data from the target point  $\mathbf{g}_{q(q)}$ , it must process the data before reaching the next target point  $\mathbf{g}_{q(q+1)}$ . The Euclidean distance between the two target points is denoted as  $D^{q(q),q(q+1)}$ . The total moving distance of the UAV to complete the inspection task is the sum of the distances of each segment along its flying path, as illustrated below

$$D^{total} = \sum_{q(1)}^{q(q)} D^{q(q),q(q+1)}. \quad (6)$$

Assuming that the UAV flies at a constant speed  $\nu$ , the time taken by the UAV swarm to travel from the current target point to the next target point is expressed as follows

$$t^{next} = D^{q(q),q(q+1)} / \nu. \quad (7)$$

The total flying time for the entire process of the UAV executing the task is represented as follows

$$t^{fly} = D^{total} / \nu. \quad (8)$$

### E. AoI Model

AoI defined in this paper aims to measure the duration from data collection to the completion of processing, incorporating waiting latency, transmission latency, and computation latency to reflect the real-time performance of DNN task execution. We assume that each UAV has a maximum memory capacity  $m_n^{threshold}$ , available energy  $e_n^{threshold}$ , and computing capacity  $f_n$ . The AoI is optimized by minimizing the UAV's moving distance and refining the DNN task assignment strategy. The waiting latency for the data collected by the leader UAV to be processed by the DNN model is denoted as

$$t_{i,n}^{wait} = T_{i'} - T_i, \quad (9)$$

where  $T_i$  represents the moment when the collected raw data is obtained on the leader UAV or when the subtask  $n$  is generated on a wingman UAV.  $T_{i'}$  signifies the moment when the collected raw data is processed on the leader UAV or when

subtask  $i$  is about to be sent from wingman UAV  $n$  to wingman UAV  $n+1$ .

The latency for the intermediate result of the completed DNN task transmitted by wingman UAV  $n$  is expressed as

$$t_{i,n}^{trans} = \frac{W_{i,l}}{r_t^{n,n+1}}, \quad (10)$$

where  $W_{i,l}$  is the data size output by the previous wingman UAV, specifically the data size before the split point  $p_{i,n'+1}$ .

The computation latency of the task is represented as

$$t_{i,n}^{comp} = \sum_{l=p_{i,n'-1}+1}^{p_{i,n'}} \frac{c_{i,l}}{f_n}, \quad (11)$$

where  $\frac{c_{i,l}}{f_n}$  denotes the computing time of the  $i$ -th subtask.  $c_{i,l}$  indicates the computing requirement of the  $i$ -th subtask, and  $f_n$  represents the computing capacity of the  $n$ -th UAV.

Therefore, the execution latency of the entire DNN task  $AoI$  and the overall system latency  $\mathcal{T}$  for the complete DNN task are as follows

$$\mathcal{T} = \sum_{i=1}^I \sum_{n=1}^N t_{i,n}^{trans} + t_{i,n}^{comp}, \quad (12)$$

$$AoI = \sum_{i=1}^I \sum_{n=1}^N t_{i,n}^{wait} + t_{i,n}^{trans} + t_{i,n}^{comp}. \quad (13)$$

#### F. Energy Consumption Model

The energy consumption of UAVs in performing DNN tasks primarily consists of computing energy consumption, transmission energy consumption, and flying energy consumption.

1) The computing energy consumption of the UAV is denoted as

$$e_n^{comp} = \sum_{i=1}^I \sum_{l=p_{i,n'-1}+1}^{p_{i,n'}} k_0 f_n^2 c_{i,l}, \quad (14)$$

where  $k_0$  represents the energy efficiency parameter and  $c_{i,l}$  denotes the computing requirement or complexity of the  $l$ -th layer in the  $i$ -th task.

2) The transmission energy consumption is approximated as the product of the transmission power  $P_n$  and the transmission time  $t_{i,n}^{trans}$  of the intermediate result of the DNN task as follows

$$e_n^{trans} = \sum_{i=1}^I P_n t_{i,n}^{trans}. \quad (15)$$

3) As one of the energy consumptions that must be considered, the flying energy consumption of the UAV is adopted in [19]. The flying energy consumption is approximated as the product  $e_n^{fly}$  of the propulsion power  $P_n^{fly}$  of the UAV and the total flying time during the task execution as follows

$$e_n^{fly} = P_n^{fly} t^{fly}, \quad (16)$$

$$P_n^{fly} = P_1 \left( 1 + \frac{3\nu^2}{\nu_{tip}^2} \right) + P_2 \left( \sqrt{1 + \frac{\nu^4}{4\nu_0^4}} - \frac{\nu^2}{2\nu_0^2} \right) + \frac{1}{2} \zeta \rho s \nu^3, \quad (17)$$

where  $P_1$  represents the blade shape power in the hovering state,  $P_2$  is the induced power,  $\nu_{tip}$  is the speed of the rotor blade tip, and  $\nu_0$  is the average induced rotor speed in the hovering state. Additionally,  $\zeta$ ,  $\rho$ ,  $s$ , and  $s$  refer to the fuselage drag ratio, air density, solidity of the rotor, and disk area, respectively. Under hovering conditions, the power consumption of the UAV is the sum of  $P_1$  and  $P_2$ .

Consequently, the energy consumption of a wingman UAV is  $e_n = e_n^{comp} + e_n^{trans} + e_n^{fly}$ . And then the total energy consumption of all DNN tasks executed by the UAV swarm is denoted as

$$E = \sum_{n=1}^N e_n^{comp} + e_n^{trans} + e_n^{fly}. \quad (18)$$

## IV. Problem formulation

In this paper, AoI and load balancing are comprehensively considered in the DNN task assignment of UAV swarms. Generally, completing tasks solely by UAVs is a common method to enhance AoI. However, this approach often leads to a significant increase in the energy consumption of individual UAVs, thereby reducing the overall survival time of the UAV swarm. To optimize load balancing in task assignment, frequent DNN task transfers within the UAV swarm may also extend task execution time and potentially deteriorate the timeliness of the collected data. Therefore, during the task execution process, it is essential to establish a reasonable DNN task partitioning and an assignment scheme that effectively balances task completion rate  $\eta = l_{\kappa}^{completed}/l_{\kappa}$ , AoI, and load balancing to improve the stability of the UAV swarm.

To this end, this paper defines a utility function  $U$  for DNN task assignment, which includes three components: the utility  $u_1$ , representing the contribution of a single UAV to a specific task; the utility  $u_2$ , which reflects the task completion rate and emphasizes the importance of both completing the task and improving the AoI; and the UAV load balancing utility  $u_3$ , indicating the variance of the remaining energy of the UAVs. This last component is crucial for maintaining balanced energy consumption across the UAV swarm.

$$U = \delta u_1 + \varepsilon u_2 + \theta u_3, \quad (19)$$

$$u_1 = e_n^{comp} + e_n^{trans}, \quad (20)$$

$$u_2 = \begin{cases} \alpha \eta_{\kappa} - \beta AoI_i, & \text{task is completed} \\ \gamma (l_{\kappa}^{completed}) - \beta \tau_i^{max}, & \text{otherwise} \end{cases}, \quad (21)$$

$$u_3 = \sum_{n=1}^N \left\{ e_n^{threshold} - e_n - \left[ \sum_{n=1}^N e_n^{threshold} - e_n \right] / N \right\}^2, \quad (22)$$

where  $\alpha, \beta, \gamma, \delta, \varepsilon, \theta$  are weight coefficients,  $l_{\kappa}^{completed}$  indicates the number of layers of the  $\kappa$ -th DNN model that have been completed.

Considering the constraints related to the number of UAVs, cache capacity, energy consumption, and latency, we

reformulate the optimization problem of DNN task assignment into determining the task split point  $p_{i,n}$  and the number of wing man UAVs  $n$  that correspond to the task. The optimization objective function  $\mathbb{P}_1$  is defined as follows

$$\max_{n, p_{i,n'}} U \quad (23)$$

$$\text{s.t. } C_1: 1 \leq p_{i,1} < p_{i,2} < \dots < p_{i,N-1} \leq L-1 \quad (23a)$$

$$C_2: 1 \leq n \leq N \quad (23b)$$

$$C_3: \sum_{l=p_{i,n'}-1+1}^{p_{i,n'}} m_{i,l} \leq m_n^{\text{threshold}} \quad (23c)$$

$$C_4: e_n^{\text{comp}} + e_n^{\text{trans}} + e_n^{\text{fly}} \leq e_n^{\text{threshold}} \quad (23d)$$

$$C_5: e_n^{\text{rendez}} \leq e_n^{\text{threshold}} - e_n \quad (23e)$$

$$C_6: \sum_{q=1}^{\mathbb{W}} \varphi_q = 1 \quad (23f)$$

$$C_7: t_{i,n}^{\text{wait}} + t_{i,n}^{\text{trans}} + t_{i,n}^{\text{comp}} \leq \tau_i \quad (23g)$$

where  $C_1$  signifies that the DNN model split point is located within the hierarchy.  $C_2$  indicates that the number of unloaded tasks falls within the total number of UAVs.  $C_3$  specifies that the task size does not exceed the maximum cache capacity of the UAV.  $C_4$  ensures that the total energy consumed does not exceed the UAV's energy capacity.  $C_5$  denotes that the remaining energy consumption of the UAV is greater than the energy consumption  $e_n^{\text{rendez}}$  required for returning.  $C_6$  requires that the leader UAV starts from the initial point and visits at least one target point.  $C_7$  stipulates that each task must not exceed the maximum allowable latency.

As shown in the previous section, the optimization objective function  $\mathbb{P}_1$  is an NP-hard problem that involves both discrete and continuous variables. Next, Problem  $\mathbb{P}_1$  is divided into a path planning subproblem and an MDP subproblem, and then solved using the proposed GDM-MADDPG with a path planning approach.

## V. Path planning method based on greedy algorithm

The greedy algorithm is employed to optimize the UAV's path due to its low computational cost and fast convergence [3]. A stochastic component is introduced to the greedy algorithm, which considers the task size within the target area, thereby providing an approximate solution for the globally optimal UAV flight path.

### A. Fitness Function

This paper employs a greedy algorithm to minimize the total flying distance of the UAV while jointly considering the task size of the target area to address the UAV path planning problem. Prior to executing DNN task assignment, the UAV must plan an optimal flying path to reduce task completion time and energy consumption. Given that the task sizes of each target area vary, we denote the task size of the  $q$ -th target point as  $\mathbb{L}_q$ , and let  $v_q$  represent the average rate at which the

UAV swarm processes tasks. Consequently, the time required to process the task size at the  $q$ -th target point is denoted as

$$t_q = \mathbb{L}_q / v_q. \quad (24)$$

To enhance overall task processing efficiency and AoI, the UAV swarm is required to complete the task after inspecting the target point and before reaching the next target point, thus establishing the condition  $t_q \leq t^{\text{next}}$ . Additionally, we define  $\Delta t = t^{\text{next}} - t_q$  as the difference between the flying time and the task processing time between two task target points.

Accordingly, the fitness function integrates the UAV flying distance and the quantity of tasks processed by the DNN model, represented as

$$F = \vartheta D^{\text{total}} + \rho \Delta t, \quad (25)$$

where  $\vartheta$  and  $\rho$  are weight coefficients utilized to balance the trade-off between the UAV flying distance and the amount of data processed by the DNN model.

---

### Algorithm 1: Path planning method based on greedy algorithm

---

**Input:** Coordinates of targets, task size of target points

$\ell_q$

**Output:** The sequence of the UAV inspection target points

- 1 Initial parameters of Path planning, such as  $\widetilde{\mathbb{W}}$ ,  $\vartheta$ ,  $\rho$ ,  $k$ ,  $v$ ,  $f_q$
- 2 Execute fitness function as Eq. (25)
- 3 Select the first target point

$$q(1) = \arg \max_{q(q) \in \widetilde{\mathbb{W}}} \left( \frac{\mathbb{L}_q}{D_{q(q), q(0)}} \right)$$

```

4 for  $i = 1, 2, \dots, q$  do
5   if  $|\widetilde{\mathbb{W}}| \leq k$  then
6      $\tilde{g} = \widetilde{\mathbb{W}}$ 
7   else
8      $\tilde{g} \subset \widetilde{\mathbb{W}}$ 
9   end
10 end
```

---

### B. Path Planning Method

The greedy algorithm is a straightforward, lightweight heuristic solution method that is easy to implement. Its fundamental principle involves making the best choice at each step based on the current state, with the aim of achieving a global optimal solution through a series of local optimal solutions [3]. However, this approach can lead to suboptimal outcomes, as selecting local optimal solutions does not guarantee a global optimal solution. To address this limitation, this paper incorporates randomness into the design of the greedy algorithm to mitigate the risk of converging on a local optimal solution.

Specifically,  $k$  candidate target points are randomly selected from the set of uninspected target points, denoted as  $\widetilde{\mathbb{W}}$ . If  $|\widetilde{\mathbb{W}}| \leq k$  indicates that all uninspected target points are chosen as candidate target points  $k$ , then we define this

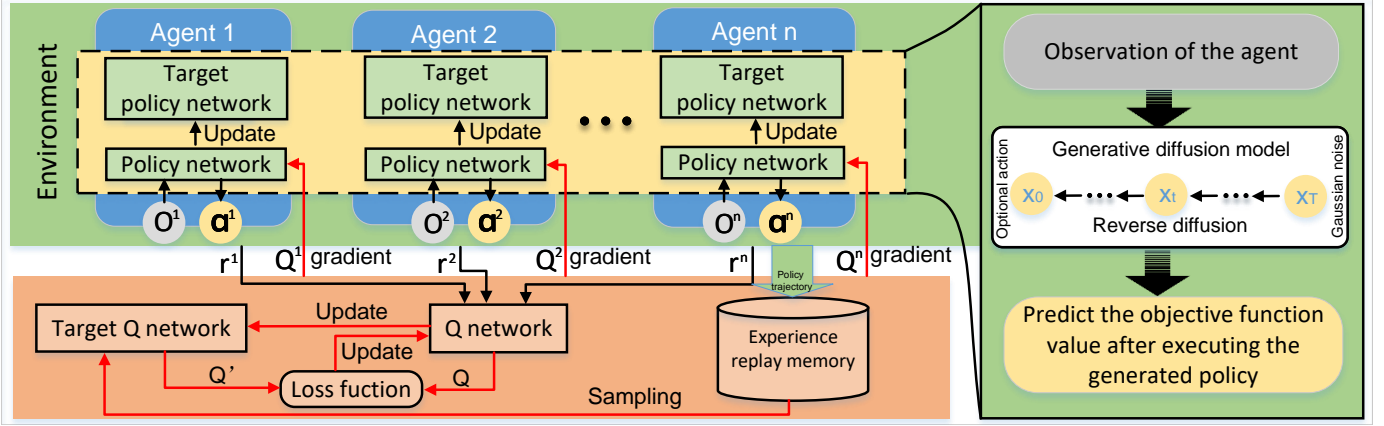


Fig. 4. GDM-MADDPG for strategy generation of DNN task assignment.

set as  $\tilde{g} = \tilde{W}$ . Otherwise,  $\tilde{W}$  uninspected target points  $k$  are randomly selected from  $\tilde{g} \subset \tilde{W}$ . For each candidate target point, the fitness function value  $F$  is calculated, and the target point with the smallest  $F$  value is selected as the next target point. A smaller  $F$  value corresponds to a lower total cost. The chosen target point is then added to the flying path sequence and removed from the candidate target point set. This process is repeated until all target points have been inspected once, at which point the UAV returns to the initial target point.

The path planning algorithm based on the greedy algorithm is illustrated in Algorithm 1. In this context, the path planning problem is denoted as  $\mathbb{P}_2$

$$\min F \quad (26)$$

$$\text{s.t. } C_8 : t_q \leq t^{\text{next}} \quad (26a)$$

where  $C_8$  signifies the requirement that the UAV swarm completes the task at the previous target point before proceeding to the next target point.

## VI. DNN task assignment algorithm based on GDM-MADDPG

GDM demonstrates robust generative capabilities and is adept at navigating complex dynamic decision optimization scenarios. Notably, it can identify optimal solutions even in the absence of a dedicated dataset. This section focuses on the design methodology and algorithmic framework of the GDM-MADDPG method. It also encompasses the design and modeling of both the diffusion reverse denoising process and MDP.

### A. Design process of GDM-MADDPG algorithm

Task assignment decision generation differs from traditional applications of GDM, primarily because decision optimization often lacks a large, dedicated dataset for offline training. In this paper, the DNN task assignment decision process involves the GDM predicting noise distribution through iterative refinement, followed by training its reverse denoising process, specifically denoising Gaussian noise to yield optimal

action decisions. This training enables the agent to execute the generated actions within the environment. The agent then fine-tunes its network parameters based on received rewards, thereby enhancing its action decision generation capabilities. This approach transforms the challenge of limited datasets into an opportunity for dynamic online learning and agent self-optimization. Building on these principles, the design process encompasses the following steps

**Agent Environment Design:** The types of tasks and data sizes at various target points are heterogeneous and subject to dynamic changes. GDM is crafted to generate optimal assignment actions, including split point selection and task selection, based on the observations of a given agent.

**Action Space Design:** The action space is established by applying a series of denoising steps on Gaussian noise via GDM, with the action vector's dimension corresponding to the number of tasks.

**Utility Function Design:** The objective is to derive action strategies for DNN task assignment through GDM, specifically targeting optimal solutions related to aspects such as AoI, load balancing, and energy consumption.

**Model Training Design:** This step focuses on training the action network to enable the agent to produce specific actions based on observations in the designated environment, all with the aim of maximizing the utility function.

### B. Reverse denoising process of GDM

The inverse denoising process of GDM serves as a reverse denoising technique that reconstructs original data from noisy observations. In this context, the denoising network, once fully trained, is capable of generating optimal decisions for DNN task assignment in any dynamic environment. Both the selection of assignment modes and the design of utility functions typically adapt to the dynamic variations present in the environment. This capability to respond to changing conditions and generate appropriate actions is invaluable in decision optimization. Consequently, the inverse denoising process of the GDM can leverage information such as the UAV observation space  $O$ , task data size  $\ell_q$ , and task type  $\kappa$  as conditions within the denoising network, thereby facilitating adaptive decision generation.



For the agent  $n$ , the objective of the inverse process is to infer the probability distribution  $\mathbf{x}_0^n$  of each task being selected from the Gaussian noise  $\mathbf{x}_T^n \sim N(0, I)$ . If the inverse distribution  $p(\mathbf{x}_{t-1}|\mathbf{x}_t)$  can be learned, it becomes possible to sample  $\mathbf{x}_t$  from the standard normal distribution  $N(0, I)$  and subsequently obtain samples from  $p(\mathbf{x}_0)$  through the inverse process. However, statistical estimation  $p(\mathbf{x}_{t-1}|\mathbf{x}_t)$  requires calculations that involve the complexity of the data distribution, which is often challenging to manage in practice. Therefore, our goal is to estimate  $p(\mathbf{x}_{t-1}|\mathbf{x}_t)$  using the parameterized model  $p_\theta$  as outlined below

$$p_\theta(\mathbf{x}_{t-1}|\mathbf{x}_t) = \mathcal{N}(\mathbf{x}_{t-1}; \boldsymbol{\mu}_\theta(\mathbf{x}_t, t), \boldsymbol{\Sigma}_\theta(\mathbf{x}_t, t)). \quad (27)$$

In this manner, we can derive the trajectory from  $\mathbf{X}_T$  to  $\mathbf{x}_0$

$$p_\theta(\mathbf{x}_{0:T}) = p_\theta(\mathbf{x}_T) \prod_{t=1}^T p_\theta(\mathbf{x}_{t-1}|\mathbf{x}_t). \quad (28)$$

By conditioning the model at time slot  $t$ , it can learn to predict the parameters of the Gaussian distribution, specifically the mean  $\boldsymbol{\mu}_\theta(\mathbf{x}_t, t)$  and covariance matrix  $\boldsymbol{\Sigma}_\theta(\mathbf{x}_t, t)$  at each time step.

The training of GDM involves optimizing the negative log-likelihood of the training data. According to the literature [50], by incorporating conditional information  $g$  in the denoising process, it can be modeled as a noise prediction model with the covariance matrix fixed to  $p_\theta(\mathbf{x}_{0:T})$ .

$$\boldsymbol{\Sigma}_\theta(\mathbf{x}_t, g, t) = \beta_t I. \quad (29)$$

The construction of the mean is as follows

$$\boldsymbol{\mu}_\theta(x_t, g, t) = \frac{1}{\sqrt{\alpha_t}} \left( x_t - \frac{\beta_t}{\sqrt{1 - \alpha_t}} \epsilon_\theta(x_t, g, t) \right). \quad (30)$$

We first sample  $\mathbf{x}_T$  from  $N(0, I)$  and then sample  $\mathbf{x}_{t-1}|\mathbf{x}_t = \frac{\mathbf{x}_t}{\sqrt{\alpha_t}} - \frac{\beta_t}{\sqrt{\alpha_t(1-\alpha_t)}} \epsilon_\theta(x_t, g, t) + \sqrt{\beta_t} \epsilon$  through the inverse denoising process parameterized by  $\theta$  where  $\epsilon \sim N(0, I)$  and  $t = 1, \dots, T$ . The loss function for the model training of the denoising network is given by

$$\mathcal{L}_t = \mathbb{E}_{\mathbf{x}_0, t, \epsilon} [\|\epsilon - \epsilon_\theta(\sqrt{\alpha_t} \mathbf{x}_0 + \sqrt{1 - \alpha_t} \epsilon, t)\|^2]. \quad (31)$$

### C. MDP modeling

GDM effectively addresses challenges within the DNN task pipeline assignment environment, generating optimal assignment decisions that maximize the utility function. This method showcases GDM's capability to manage complex data distributions and produce high-quality decisions, particularly in dynamic and evolving environments [8]. By integrating DRL, more efficient and adaptable action strategies can be developed. Consequently, the utility maximization problem is formulated as a multi-agent Markov decision process (MDP), represented by a tuple  $(n, O, \mathcal{A}, r, \gamma)$ , where  $n$  denotes the number of agents,  $O$  is the observation space of the agent,  $\gamma$  represents the discount factor, and  $r$  signifies the reward obtained by the agent. The agent is represented by the UAV. It learns an optimal task assignment strategy based on GDM-MADDPG according to task size, computing resources, and

task latency to achieve optimal load balancing and AoI. The DNN task assignment decision generation based on GDM-MADDPG is detailed in Fig. 4 and Algorithm 2.

---

### Algorithm 2: GDM-MADDPG Algorithm

---

```

1 Initialize the parameters of the Critic network and the
  Actor network (denoising network)
2 for episode = 0 → ε do
3   Reset the environment and the initial observation O
4   for t = 1, 2, ..., T do
5     for n = 1, 2, ..., N do
6       Use the observation space of agent n as a
        condition of denoising network to generate
        adapted actions
7       for t = 1, 2, ..., T do
8         Predict the noise ε
9         Gaussian noise x_T is denoised in
            reverse process, obtaining x_0^n
10        Agent n selects an action x_0^n according
            to a_t^i = f(x_0^i)
11        Execute the chosen action a_t^i
12        Obtain the reward x_0^n and the next
            observation o_t^{n'}
13        o_t^n ← o_t^{n'}
14        if the buffer is not full then
15          Store the training data
            ((O_t, A_t, R_t, O_t^i)) into the buffer
16        else
17          Update the experience replay buffer
18        end
19      end
20    for n = 1, 2, ..., N do
21      b samples are taken from the buffer
            (O_j, A_j, R_j, O_j^i), ∀ j = 1, 2, ..., T
22      Calculate the target value
23      Minimize the loss function to update
            the parameters of the Critic network
24      Update the Actor and Critic target
            network parameters for each agent
            according to Eq. (31)
25    end
26  end
27 end
28 end

```

---

**Observation Space:** In each time slot  $t$ , the UAV collects observations from its environment. The observation space is denoted as  $O_t = \{o_t^1, o_t^2, \dots, o_t^N\}$ , with the observation of a single agent represented by

$$o_t^n = \{\ell_t, \kappa_t, l_{\kappa, t}^{\text{completed}}, \tau_t, \mathbf{e}_t, \mathbf{m}_t, \mathcal{P}_t, \mathbf{q}(q)\}, \quad (32)$$

where  $\ell_t$  indicates the amount of data associated with the DNN task at time slot  $t$ ,  $\kappa_t$  represents the type of DNN model,  $l_{\kappa, t}^{\text{completed}} = \{l_1^{\text{completed}}, l_2^{\text{completed}}, \dots, l_l^{\text{completed}}\}$  indicates the degree of completion of the DNN task (i.e., the number of completed layers),  $\tau_i^{\text{max}} = \{\tau_1^{\text{max}}, \tau_2^{\text{max}}, \dots, \tau_T^{\text{max}}\}$  denotes the maximum latency that each task can tolerate at time slot  $t$ ,

TABLE II  
EXPERIMENT PARAMETERS

Parameters	Values
Number of UAV $N$	[5, 10]
Number of DNN types $\mathbb{K}$	[1, 3]
Number of target points $\mathbb{W}$	[10, 50]
Size of task $\mathbb{L}_{\mathbb{W}}$	[0, 80] GB
Number of random $k$	5
Weight of distance $\vartheta$	0.5
Weight of task size $\rho$	0.5
UAV propulsion speed $\nu$	20m/s
Average task processing rate $v_q$	10GB/min
Computational complexity $c$	[50, 500] cycle/bit
Maximum transmission power $P_n$	[50, 100] mW
Maximum bandwidth $B_n$	[1, 5] MHz
Maximum cache resources $m$	[100, 500] GB
Maximum tolerable latency $\tau$	[10, 200] ms
Noise power $P_N$	-115 dBm
Computing capacity of UAV $f_n$	15 Gigacycles/s

$e_t$  represents the energy consumption constraint of the UAV (the remaining energy at time slot  $t$ ,  $m_t$  indicates the memory constraint of the UAV (the remaining memory at time slot  $t$ ),  $\mathcal{P}_t = \{\mathcal{P}_t^1, \mathcal{P}_t^2, \dots, \mathcal{P}_t^n\}$  represents the positions of all UAVs at time slot  $t$ , and  $q_t(q)$  signifies the positions of all target points.

**Action Space:** The action space is defined as  $\mathcal{A}^n = \{a_1^n, a_2^n, \dots, a_t^n\}$ . In each time slot  $t$ , the agent's action is denoted by  $a_t^i$ , where  $i = \{1, 2, \dots, I\}$  represents the task chosen by the agent for execution, and  $a_t^n = \{a_t^1, a_t^2, \dots, a_t^I\}$  signifies the action taken.

**Reward Function:** The agent's actions are constrained by AoI and are closely related to load balancing and task completion rates. To maximize the system utility, the agent observes  $o_t^n$  and executes action  $a_t^i$  to obtain the reward  $r_t^n$  as follows

$$r_t^{n,indiv} = \begin{cases} \delta u_1, e_n^{threshold} - e_n \geq e^{rendez} \\ -\sigma(e_n^{threshold} - e_n), otherwise \end{cases}, \quad (33)$$

$$r_t^{n,group} = \varepsilon u_2 + \theta u_3, \quad (34)$$

$$r_t^n = \vartheta r_t^{n,indiv} + (1 - \vartheta) r_t^{n,group}, \quad (35)$$

where  $r_t^{n,indiv}$  and  $r_t^{n,group}$  represent individual and global rewards, respectively.  $\sigma$  and  $\vartheta$  are weight coefficients, and  $e^{rendez}$  denotes the energy consumption required for the UAV to return.

## VII. Experiment setup and performance evaluation

To assess the efficacy of the proposed DNN task assignment algorithm, we conduct numerical experiments and analyze its performance. This analysis includes a comparison with several benchmark algorithms to demonstrate its effectiveness and advantages.

### A. Experiment setup

#### 1) Training environment and network

The hardware configuration consists of an Intel i7-13700K CPU and an NVIDIA RTX 4090 with 24 GB of RAM. The software environment includes pytorch GPU version 1.11.0 and Python version 3.8. The parameters for DNN are specified as follows: for the Actor network, the number of neurons in the first and second hidden layers are set to 256, respectively, while the number of neurons in the third hidden layer is determined by the dimensionality of possible actions. For the Critic network, the neuron counts for the three hidden layers are set to 256, respectively. During training, the learning rates for the Actor and Critic networks are set to  $\gamma = 10^{-3}$ . The mini-batch size during training is 512. The discount factor is set to  $\gamma_m = 0.9$ , and the initial value and decay rate for exploration are defined as  $\epsilon_0 = 0.9$  and  $\beta = 10^{-4}$ , respectively.

In our simulation, we examine the performance of collaborative DNN task assignment across different data sizes. To simplify calculations, we assume a constant transmission model, where the data transmission rate remains uniform during a complete collaborative task assignment. The experimental parameters and their corresponding values are detailed in Table II [51].

#### 2) Simulation scenario

We perform simulations under the following scenario: one airship positioned at an altitude of 10 km, accompanied by nine UAVs at an altitude of 3 km, covering an area of  $12 \times 12$  km<sup>2</sup>. The airship is located at the center of this area, while the leader UAV and wingman UAVs are uniformly distributed throughout it. The airship obtains the mission directives from the ground control center, formulates the optimal flight sequence for the designated mission targets, and transmits the planned route information to the lead aircraft. The lead aircraft, along with several wingmen UAV, then executes a coordinated flight along the predetermined route. It is important to note that all UAVs fall within the coverage area of the airship and are interconnected and capable of communicating with one another. Additionally, considering overall accuracy in detecting target amounts, the Yolov5 model outperforms all seven attention-optimized Yolov5 variants as well as other state-of-the-art object detection models [4]. In this study, we employ Yolov5 as the DNN inference task model and conduct comparative testing experiments that focus on AoI, load balancing, and system stability to evaluate the effectiveness of the proposed method.

#### 3) Benchmark algorithms

To demonstrate the advantages of the proposed method, we examine the following benchmark algorithms. To ensure a fair comparison, the structures and parameters of the deep neural networks (DNNs) are standardized. **MADDPG** is a policy-based reinforcement learning method, primarily utilizing a centralized training and distributed execution framework. It extends single-agent reinforcement learning algorithms from the actor-critic framework to accommodate multi-agent scenarios [41]. **MADDPG with path planning** integrates the optimal path planning approach presented in this paper with

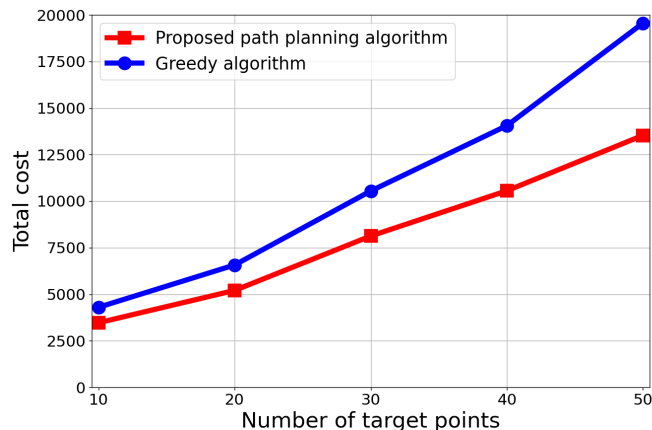


Fig. 5. Total cost of path planning under different target points.

MADDPG, facilitating the generation of task assignment decisions that align with the requirements for task execution.

## B. Performance evaluation

### 1) Path planning

As illustrated in Fig. 5, the cost associated with the UAV's optimal pathfinding increases as the number of target points rises. Notably, the path planning algorithm proposed in this study consistently exhibits lower costs compared to the greedy algorithm across all evaluated scenarios. Specifically, for target point counts of 10, 20, 30, 40, and 50, the total cost produced by the proposed algorithm is reduced by approximately 19.3%, 21.1%, 23.0%, 25.6%, and 27.1% respectively, in comparison to the greedy algorithm. This enhancement can be attributed to the expanding solution space that accompanies an increase in the number of target points. As the candidate set of target points grows, the proposed algorithm is afforded greater opportunities to explore solutions that yield lower total costs, ultimately facilitating the identification of the optimal path with the minimal total cost. Thus, it is evident that the algorithm developed in this study is particularly adept at addressing path planning challenges that involve a larger number of target points.

This experiment simulated a UAV inspection area consisting of eight target points, each defined by a distinct task size, as illustrated in Fig. 6. The experimental results are illustrated in Fig. 6a depicts the UAV path planning method based on the greedy algorithm we proposed. By comprehensively considering both task size and flying path, this method generates the global optimal UAV flying path and target point sequence, prioritizing target points with larger task sizes while ensuring coverage of all target points. Conversely, Fig. 6b presents a greedy algorithm that does not incorporate a random selection strategy. This approach, which selects the best option at each step based solely on the current state, is prone to local optima. As a result, it can lead to a significant increase in flying path length, reducing the survival time of the UAV swarm and hindering its ability to conduct long-term operations under energy constraints.

### 2) Training Procedures

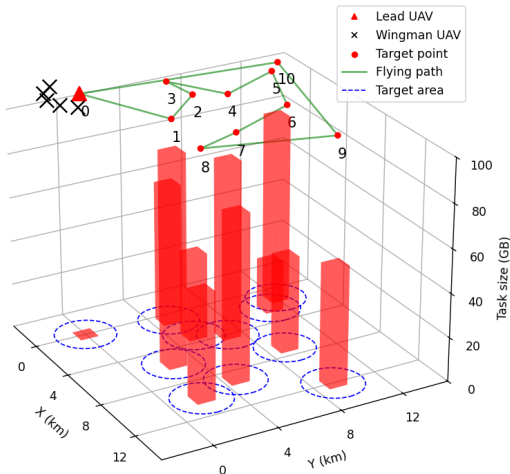
We conduct ten independent training runs for each algorithm. As illustrated in Fig. 7, although the proposed DM-MADDPG converges at a slower rate than the two algorithms, DM-MADDPG demonstrates superior performance compared to the other solutions. The total reward attained by DM-MADDPG increases throughout the training process, eventually converging to approximately 5000 after around 600 training episodes. This enhancement is attributed to the generative capabilities of GDM, which markedly improve action sample efficiency by progressively reducing noise through multiple denoising steps. Finally, the low performance of the two algorithm, further highlighting the effectiveness of the proposed GDM-MADDPG method.

By conducting a series of systematic experiments, we aim to identify the optimal values for two key parameters that influence the performance of MADDPG algorithm: 1) learning rate and 2) batch size. The experimental results, illustrated in Fig. 8a, clarify the convergence behavior of the reward function under varying learning rates. A learning rate of 0.01 is excessively large, preventing convergence even after 1000 training iterations. Similarly, learning rates of 0.0001 is not facilitate convergence. Notably, the 0.001 learning rate promotes faster convergence. The suitable learning rate of 0.001 is employed to assess the effects of different batch size on training performance. As illustrated in Fig. 8b, a batch size of 512 is recognized as the most advantageous option.

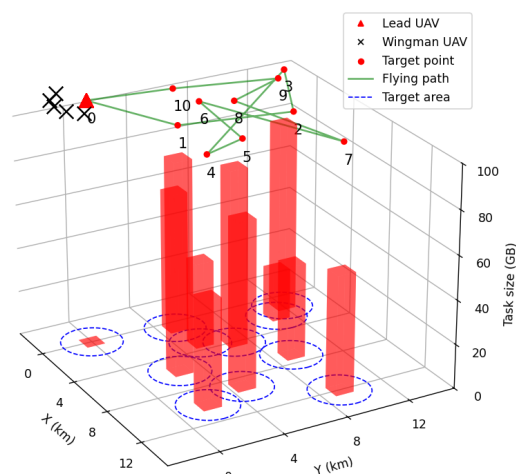
The convergence of GDM-MADDPG across various DNN model tasks is illustrated in Fig. 9. Despite the differences in structural complexity among the DNN models, the proposed method successfully accommodates these tasks and achieves convergence. The AlexNet model, characterized by fewer layers and lower computational requirements, demonstrates favorable convergence performance. In contrast, the VGG16 model, with its greater number of layers and higher computational demands, experiences increased processing delays, resulting in lower rewards and reduced convergence efficacy for our method. Although the convergence performance of our method on the YOLOv5 model is slightly inferior to that of AlexNet, YOLOv5, as a widely adopted real-time object detection algorithm, has a model complexity that lies between the two aforementioned models. Consequently, subsequent experiments employ YOLOv5 as the experimental task model to validate the superior performance of this method in terms of AOI and task completion rate.

### 3) Benchmark algorithms:

This study compares the AoI of different methods across varying task sizes, as illustrated in Fig. 10. The AoI performance of the MADDPG-based method is significantly enhanced when combined with the path planning approach. Furthermore, the GDM-MADDPG method proposed in this paper, which builds upon MADDPG and incorporates the advantages of GDM in handling complex data distributions and generating high-quality task assignment decisions, improves the timeliness and generalization ability of task assignment decision generation. This results in the generation of the most suitable task assignment decisions for the current state, thereby reducing the transmission time during serial task execution.



(a) Path planning based on a greedy algorithm with a stochastic strategy.



(b) Path planning based on a greedy algorithm without a stochastic strategy.

Fig. 6. UAV Path Planning Considering Mission Size and flying Distance.

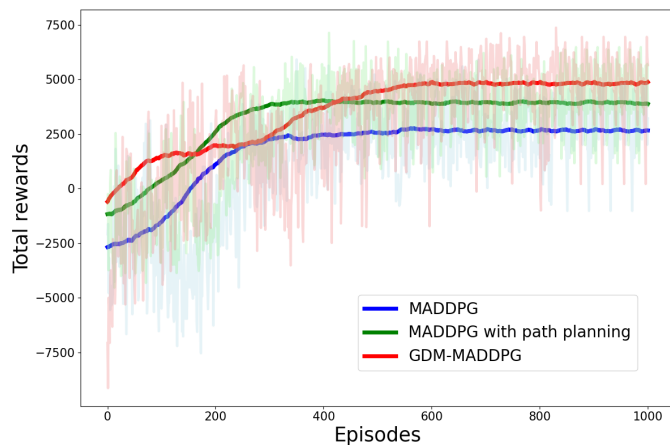
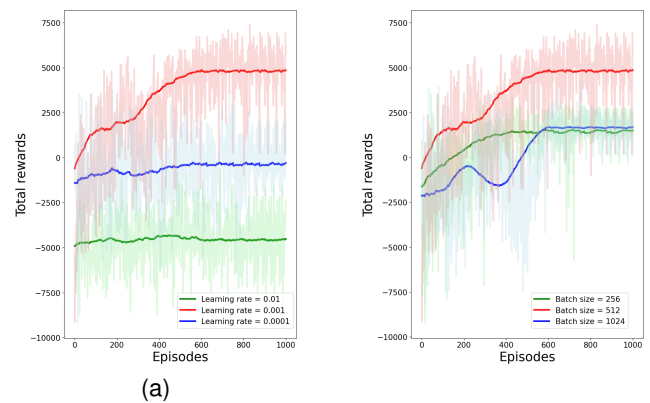


Fig. 7. The total reward from the training of different algorithms.

According to Eq. (25), this method also addresses the path planning optimization of the task target points and task sizes, which reduces the waiting delays associated with tasks and enhances the AoI performance in task completion.

The task completion rates of different methods were compared under various task sizes, as shown in Fig. 11. As the optimization focus of this study, system utility comprehensively considers energy consumption, task completion rates, AoI, and task load balancing. The method proposed in this paper outperforms other methods in optimizing system utility, indicating that the optimized task path planning and task offloading decision generation achieve a joint optimization of multiple objectives. In terms of path planning, the method not only considers the optimal route but also accounts for the task size requests at the target points, enhancing the selectivity of local optima. Regarding DNN task assignment, factors such as task division decisions, wingman selection, and load balancing are incorporated. Additionally, the introduced GDM reverse denoising process improves the learning and



(a)

(b)

Fig. 8. The training procedures of different learning rate and batch size.

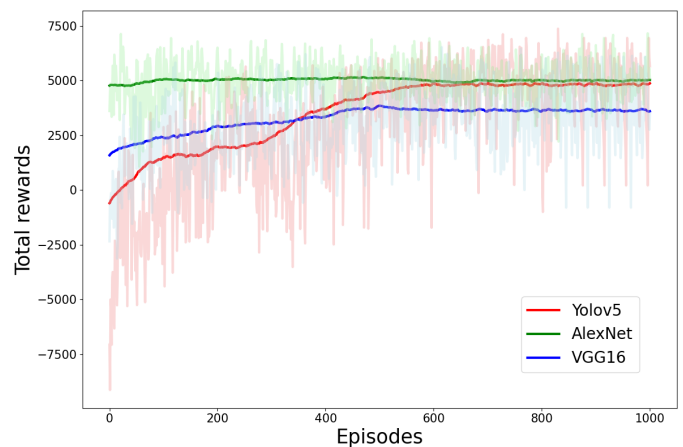


Fig. 9. The total reward from the training of different DNN models.

generation capabilities of agent decisions, leading to well-generalized action decisions. Consequently, as the task size gradually increases, the MADDPG-based decision method

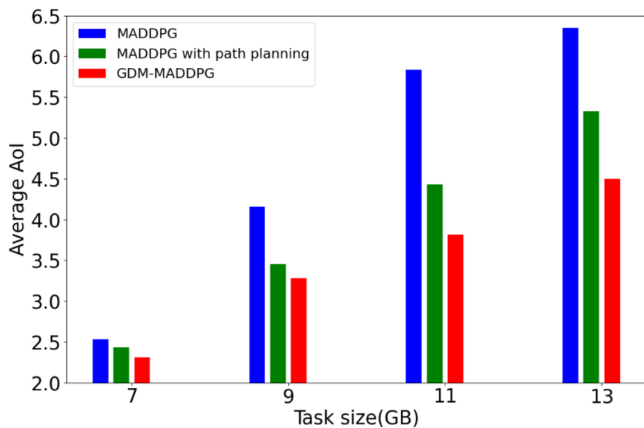


Fig. 10. The AoI of different methods across varying task sizes.

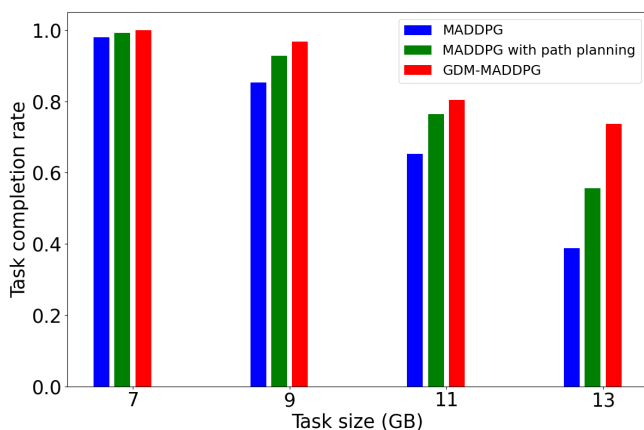


Fig. 11. The task completion rates for different task sizes.

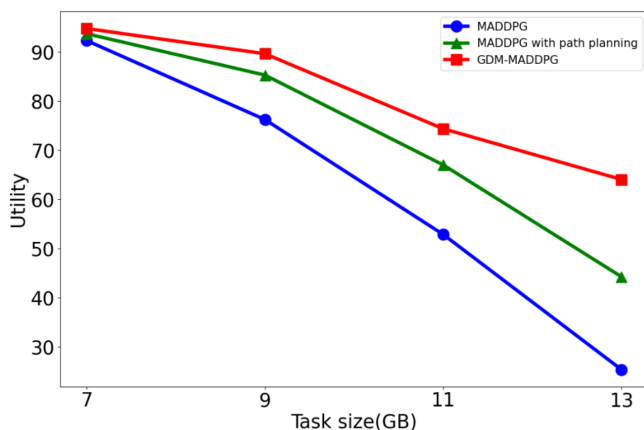


Fig. 12. The utility of different methods across varying task sizes.

lacks robust dynamic adaptability under multiple constraints. Its learning capability is constrained by the fixed learning mechanism of the actor-critic network, resulting in an absence of a strategy with generalization capabilities.

The system utility of different methods were compared under various task sizes, as shown in Fig. 12, for tasks below 7GB, the task completion rates of the various methods are similar. This is attributed to the small task sizes, as all UAVs

are isomorphic with identical processing capabilities, operating within the specified task completion delay constraints. However, as task sizes increase, the need for additional task assignment work under delay constraints arises, directly increasing waiting delays, intermediate data transmission delays, and real-time calculation delays. This results in a downward trend in task completion rates for all methods. The proposed method considers task size constraints during the path planning stage, and the task assignment decisions can be rapidly learned and generated through the GDM method, further reducing task processing delays and enabling a greater number of tasks to be completed within the specified time. Moreover, these findings indicate that the proposed method is particularly well-suited for executing large-scale tasks.

## VIII. Conclusion

In this paper, we addressed the challenge of joint flying path planning, task assignment, and load balancing in UAV networks as a two-stage optimization problem. Our primary objective is to minimize the DNN-based task AoI while maximizing the survival time of the UAV swarm. In the first stage, we consider the task size of the area to be inspected and the shortest flying path as optimization constraints. We then employ a heuristic algorithm to optimize the UAV's flying path, focusing on reducing energy consumption and minimizing flying duration. In the second stage, we introduce a novel GDM-MADDPG algorithm to determine optimal DNN task assignment decisions. Through numerical simulations, we demonstrate the superior performance of our proposed algorithm compared to existing benchmark solutions.

## References

- [1] G. Raja, A. Manoharan, and H. Siljak, "Ugen: Uav and gan-aided ensemble network for post-disaster survivor detection through oran," *IEEE Transactions on Vehicular Technology*, 2024.
- [2] T. Wang, X. Huang, Y. Wu, L. Qian, B. Lin, and Z. Su, "Uav swarm-assisted two-tier hierarchical federated learning," *IEEE Transactions on Network Science and Engineering*, 2023.
- [3] B. Tian, L. Wang, L. Xu, W. Pan, H. Wu, L. Li, and Z. Han, "Uav-assisted wireless cooperative communication and coded caching: a multiagent two-timescale drl approach," *IEEE Transactions on Mobile Computing*, 2023.
- [4] Y. Xiong, X. Zeng, W. Lai, J. Liao, Y. Chen, M. Zhu, and K. Huang, "Detecting and mapping individual fruit trees in complex natural environments via uav remote sensing and optimized yolov5," *IEEE Journal of Selected Topics in Applied Earth Observations and Remote Sensing*, 2024.
- [5] Y. Gao, Y. Xiao, M. Wu, M. Xiao, and J. Shao, "Dynamic social-aware peer selection for cooperative relay management with d2d communications," *IEEE Transactions on Communications*, vol. 67, no. 5, pp. 3124–3139, 2019.
- [6] M. Wu, G. Cheng, P. Li, R. Yu, Y. Wu, M. Pan, and R. Lu, "Split learning with differential privacy for integrated terrestrial and non-terrestrial networks," *IEEE Wireless Communications*, 2023.
- [7] T. Wang, Y. Li, and Y. Wu, "Energy-efficient uav assisted secure relay transmission via cooperative computation offloading," *IEEE Transactions on Green Communications and Networking*, vol. 5, no. 4, pp. 1669–1683, 2021.
- [8] Z. Liu, H. Du, J. Lin, Z. Gao, L. Huang, S. Hosseinalipour, and D. Niyato, "Dnn partitioning, task offloading, and resource allocation in dynamic vehicular networks: A lyapunov-guided diffusion-based reinforcement learning approach," *arXiv preprint arXiv:2406.06986*, 2024.

- [9] H. Sun, Y. Qu, C. Dong, H. Dai, Z. Li, L. Zhang, Q. Wu, and S. Guo, "All-sky autonomous computing in uav swarm," *IEEE Transactions on Mobile Computing*, 2024.
- [10] C. Deng, X. Fang, and X. Wang, "Integrated sensing, communication, and computation with adaptive dnn splitting in multi-uav networks," *IEEE Transactions on Wireless Communications*, 2024.
- [11] Y. Qu, H. Sun, C. Dong, J. Kang, H. Dai, Q. Wu, and S. Guo, "Elastic collaborative edge intelligence for uav swarm: Architecture, challenges, and opportunities," *IEEE Communications Magazine*, 2023.
- [12] M. Jouhari, A. K. Al-Ali, E. Baccour, A. Mohamed, A. Erbad, M. Guizani, and M. Hamdi, "Distributed cnn inference on resource-constrained uavs for surveillance systems: Design and optimization," *IEEE Internet of Things Journal*, vol. 9, no. 2, pp. 1227–1242, 2021.
- [13] C. Wang, B. Carlson, and Q. Han, "Object recognition offloading in augmented reality assisted uav-ugv systems," in *Proceedings of the Ninth Workshop on Micro Aerial Vehicle Networks, Systems, and Applications*, 2023, pp. 33–38.
- [14] M. Zhao, X. Zhang, Z. Meng, and X. Hou, "Reliable dnn partitioning for uav swarm," in *2022 International Wireless Communications and Mobile Computing (IWCMC)*. IEEE, 2022, pp. 265–270.
- [15] T. Yang, H. He, and L. Kong, "Multi-uav maritime search and rescue with dnn inference acceleration," in *2023 International Conference on Ubiquitous Communication (Ucom)*. IEEE, 2023, pp. 248–253.
- [16] Y. Long, S. Zhao, S. Gong, B. Gu, D. Niyato, and X. Shen, "Aoi-aware sensing scheduling and trajectory optimization for multi-uav-assisted wireless backscatter networks," *IEEE Transactions on Vehicular Technology*, 2024.
- [17] W. Ren, Y. Qu, Z. Qin, C. Dong, F. Zhou, L. Zhang, and Q. Wu, "Efficient pipeline collaborative dnn inference in resource-constrained uav swarm," in *2024 IEEE Wireless Communications and Networking Conference (WCNC)*. IEEE, 2024, pp. 1–6.
- [18] S. Lins, K. V. Cardoso, C. B. Both, L. Mendes, J. F. De Rezende, A. Silveira, N. Linder, and A. Klautau, "Artificial intelligence for enhanced mobility and 5g connectivity in uav-based critical missions," *IEEE Access*, vol. 9, pp. 111 792–111 801, 2021.
- [19] W. Liu, B. Li, W. Xie, Y. Dai, and Z. Fei, "Energy efficient computation offloading in aerial edge networks with multi-agent cooperation," *IEEE Transactions on Wireless Communications*, vol. 22, no. 9, pp. 5725–5739, 2023.
- [20] X. Huang, Y. Zhang, Y. Qi, C. Huang, and M. S. Hossain, "Energy-efficient uav scheduling and probabilistic task offloading for digital twin-empowered consumer electronics industry," *IEEE Transactions on Consumer Electronics*, 2024.
- [21] M. Ma, Z. Wang, S. Guo, and H. Lu, "Cloud-edge framework for aoi-efficient data processing in multi-uav-assisted sensor networks," *IEEE Internet of Things Journal*, 2024.
- [22] Y. Wang, J. Fang, Y. Cheng, H. She, Y. Guo, and G. Zheng, "Cooperative end-edge-cloud computing and resource allocation for digital twin enabled 6g industrial iot," *IEEE Journal of Selected Topics in Signal Processing*, 2023.
- [23] J. Tian, L. Zhu, F. R. Yu, H. Wang, and T. Tang, "Optimizing edge resources in intelligent railway construction: A two-level game approach," *IEEE Transactions on Vehicular Technology*, 2024.
- [24] X. Wang, L. Wang, Z. Liu, L. Xu, and A. Fei, "On uav serving nodes trajectory planning for fast localization in forest environment: A multi-agent drl approach," in *2023 IEEE Wireless Communications and Networking Conference (WCNC)*. IEEE, 2023, pp. 1–6.
- [25] Y. Gao, Y. Xiao, M. Wu, M. Xiao, and J. Shao, "Game theory-based anti-jamming strategies for frequency hopping wireless communications," *IEEE Transactions on Wireless Communications*, vol. 17, no. 8, pp. 5314–5326, 2018.
- [26] U. Nepal and H. Eslamiat, "Comparing yolov3, yolov4 and yolov5 for autonomous landing spot detection in faulty uavs," *Sensors*, vol. 22, no. 2, p. 464, 2022.
- [27] L. Zhu, S. Zhang, X. Wang, S. Chen, H. Zhao, and D. Wei, "Multilevel recognition of uav-to-ground targets based on micro-doppler signatures and transfer learning of deep convolutional neural networks," *IEEE Transactions on Instrumentation and Measurement*, vol. 70, pp. 1–11, 2020.
- [28] S. Mousavi and G. Farahani, "A novel enhanced vgg16 model to tackle grapevine leaves diseases with automatic method," *IEEE Access*, vol. 10, pp. 111 564–111 578, 2022.
- [29] M. Gao, R. Shen, L. Shi, W. Qi, J. Li, and Y. Li, "Task partitioning and offloading in dnn-task enabled mobile edge computing networks," *IEEE Transactions on Mobile Computing*, vol. 22, no. 4, pp. 2435–2445, 2021.
- [30] H. Li, X. Li, Q. Fan, Q. He, X. Wang, and V. C. Leung, "Distributed dnn inference with fine-grained model partitioning in mobile edge computing networks," *IEEE Transactions on Mobile Computing*, 2024.
- [31] C. Liu and K. Liu, "Toward reliable dnn-based task partitioning and offloading in vehicular edge computing," *IEEE Transactions on Consumer Electronics*, vol. 70, no. 1, pp. 3349–3360, 2023.
- [32] T. Mohammed, C. Joe-Wong, R. Babbar, and M. Di Francesco, "Distributed inference acceleration with adaptive dnn partitioning and offloading," in *IEEE INFOCOM 2020-IEEE Conference on Computer Communications*. IEEE, 2020, pp. 854–863.
- [33] C. Xu, S. Liu, C. Zhang, Y. Huang, Z. Lu, and L. Yang, "Multi-agent reinforcement learning based distributed transmission in collaborative cloud-edge systems," *IEEE Transactions on Vehicular Technology*, vol. 70, no. 2, pp. 1658–1672, 2021.
- [34] Z. Liu, L. Huang, Z. Gao, M. Luo, S. Hosseinalipour, and H. Dai, "Gardl: Graph neural network-augmented deep reinforcement learning for dag task scheduling over dynamic vehicular clouds," *IEEE Transactions on Network and Service Management*, 2024.
- [35] X. Liu, Y. Liu, Y. Chen, and L. Hanzo, "Trajectory design and power control for multi-uav assisted wireless networks: A machine learning approach," *IEEE Transactions on Vehicular Technology*, vol. 68, no. 8, pp. 7957–7969, 2019.
- [36] M. Kim, H. Lee, S. Hwang, M. Debbah, and I. Lee, "Cooperative multi-agent deep reinforcement learning methods for uav-aided mobile edge computing networks," *IEEE Internet of Things Journal*, 2024.
- [37] Y. Ju, Y. Chen, Z. Cao, L. Liu, Q. Pei, M. Xiao, K. Ota, M. Dong, and V. C. Leung, "Joint secure offloading and resource allocation for vehicular edge computing network: A multi-agent deep reinforcement learning approach," *IEEE Transactions on Intelligent Transportation Systems*, vol. 24, no. 5, pp. 5555–5569, 2023.
- [38] X. Li, W. Huangfu, X. Xu, J. Huo, and K. Long, "Secure offloading with adversarial multi-agent reinforcement learning against intelligent eavesdroppers in uav-enabled mobile edge computing," *IEEE Transactions on Mobile Computing*, 2024.
- [39] Y. Liu, P. Lin, M. Zhang, Z. Zhang, and F. R. Yu, "Mobile-aware service offloading for uav-assisted iovs: A multi-agent tiny distributed learning approach," *IEEE Internet of Things Journal*, 2024.
- [40] Y. Hou, Z. Wei, R. Zhang, X. Cheng, and L. Yang, "Hierarchical task offloading for vehicular fog computing based on multi-agent deep reinforcement learning," *IEEE Transactions on Wireless Communications*, 2023.
- [41] P. Qin, Y. Fu, Y. Xie, K. Wu, X. Zhang, and X. Zhao, "Multi-agent learning-based optimal task offloading and uav trajectory planning for agin-power iot," *IEEE Transactions on Communications*, vol. 71, no. 7, pp. 4005–4017, 2023.
- [42] G. Sun, W. Xie, D. Niyato, H. Du, J. Kang, J. Wu, S. Sun, and P. Zhang, "Generative ai for advanced uav networking," *arXiv preprint arXiv:2404.10556*, 2024.
- [43] Y. Li, L. Feng, Y. Yang, and W. Li, "Gan-powered heterogeneous multi-agent reinforcement learning for uav-assisted task offloading," *Ad Hoc Networks*, vol. 153, p. 103341, 2024.
- [44] Y. Gao, Z. Ye, M. Xiao, Y. Xiao, and D. I. Kim, "Guiding iot-based healthcare alert systems with large language models," *arXiv preprint arXiv:2408.13071*, 2024.
- [45] S. Zhang, A. Wijesinghe, and Z. Ding, "Rme-gan: A learning framework for radio map estimation based on conditional generative adversarial network," *IEEE Internet of Things Journal*, vol. 10, no. 20, pp. 18 016–18 027, 2023.
- [46] N. Van Huynh, J. Wang, H. Du, D. T. Hoang, D. Niyato, D. N. Nguyen, D. I. Kim, and K. B. Letaief, "Generative ai for physical layer communications: A survey," *IEEE Transactions on Cognitive Communications and Networking*, 2024.
- [47] Y. Liu, Y. Mao, Z. Liu, F. Ye, and Y. Yang, "Joint task offloading and resource allocation in heterogeneous edge environments," *IEEE Transactions on Mobile Computing*, 2023.
- [48] H. Kang, X. Chang, J. Mišić, V. B. Mišić, J. Fan, and Y. Liu, "Cooperative uav resource allocation and task offloading in hierarchical aerial computing systems: A mapo-based approach," *IEEE Internet of Things Journal*, vol. 10, no. 12, pp. 10 497–10 509, 2023.
- [49] X. Tang, X. Li, R. Yu, Y. Wu, J. Ye, F. Tang, and Q. Chen, "Digital-twin-assisted task assignment in multi-uav systems: A deep reinforcement learning approach," *IEEE Internet of Things Journal*, vol. 10, no. 17, pp. 15 362–15 375, 2023.
- [50] J. Ho, A. Jain, and P. Abbeel, "Denoising diffusion probabilistic models," *Advances in neural information processing systems*, vol. 33, pp. 6840–6851, 2020.

- [51] Y. Wang, C. Zhang, T. Ge, and M. Pan, "Computation offloading via multi-agent deep reinforcement learning in aerial hierarchical edge computing systems," *IEEE Transactions on Network Science and Engineering*, 2024.